Structural Eng. / Earthquake Eng. Vol. 5. No. 1, 173s-182s. April 1988
Japan Society of Civil Engineers (Proc. of JSCE No. 392/I-9)

SYNTHESIS OF STRONG MOTION ACCELEROGRAMS FROM SMALL EARTHQUAKE RECORDS BY USE OF A SCALING LAW OF SPECTRA

*By Makoto KAMIYAMA**

A method for synthesizing strong-motion accelerogam from small earthquake records is presented with aid of the faulting source model. It is derived by extending the spectra relation satisfied in a point source model to ones in the faulting source model. The important terms involved in the method, namely, the scaling law of source spectra and the number of sub-faults are obtained statistically from the past strong-motion accelerograms. The method is applied to several representative earthquakes occurred in Japan, and it is shown that the synthesized accelerograms by the method agree relatively well with the observed ones in the points of amplitude, duration and spectra characteristics.

Keywords: *strong-motion accelerogram, fault source model, scaling law of spectra, statistical analysis*

1. INTRODUCTION

Prediction of strong earthquake motions is quite significant in designing input motions to structures for earthquake-resistant analyses. In general, earthquake ground motions are influenced by various factors such as source characteristics, propagation path of waves and local soil layers, so it is needed to synthesize the effects due to these factors for the prediction of them. Of these factors, source characteristics have been often represented merely by earthquake magnitude in engineering field. As important contributions have been made in the past decade to understanding earthquake mechanism, however, faulting source models have been employed even in engineering to predict ground motions precisely[1]. Although various faulting source models have been proposed so far, engineers have recently focussed their attention on the so-called heterogeneous faulting models[2], because such models are useful to follow high frequency motions of acceleration which they are concerned mainly about.

When applying the heterogeneous models of fault to the prediction of ground acceleration motions, there may be two main difficulties necessary to overcome. Namely, one is that high frequency motions are affected severely by local soil conditions and therefore we need to take the fine structures of propagation path of waves into consideration as well as the detailed faulting process. The other is that the heterogeneous aspects of faulting, especially, the fault parameters controlling high frequency motions have been little known. The first of the two is such a problem that even powerful computers of today have difficulty in treating as long as purely analytical models are involved. In order to overcome this difficulty, Hartzell [3] presented a skillful idea in which small earthquake records are used as an empirical Green's function for a large earthquake faulting. This technique would be very efficient since we can predict ground

* Member of JSCE, Dr. Eng. Associate Professor, Dept. of Civil Eng., Tohoku Institute of Technology (Yagiyama-Kasumicho, Sendai 982, Japan)

motions by use of faulting models without estimating the complicated interference due to the propagation media of waves. Although Hartzell's technique was first proposed to estimate displacement motions consisting of periods over some seconds, it has also been applied to the prediction of acceleration motions because of its skillfulness[4]. Regretably, however, the technique has not succeeded satisfactorily in predicting acceleration motions. The greatest reason is that the faulting parameters intimately associated with acceleration motions have not been made clear and the method for synthesizing small earthquake records has not become valid. In other words, the second problem mentioned above is the most serious obstacle to apply Hartzell's technique to acceleration motions.

In a previous paper[5], the author has showed the general aspects of the heterogeneity over earthquake fault and derived a simplified scaling law of acceleration source spectra with aid of statistical analyses for strong-motion accelerograms obtained in Japan. Based on these results, the present paper deals with a method of predicting strong-motion accelerograms from small earthquake records.

As for Hartzell's technique, several workers have recently applied it to acceleration motions [6), 7)]. Their methods are mostly due to the synthesis of accelerograms in time domain, making use of scaling laws of fault described by earthquake moment. In contrast with these studies, the present research, which is most characterized by simplicity, employs the spectral synthesis determined statistically in terms of earthquake magnitude.

2. A METHOD FOR SYNTHESIZING ACCELEROGRAMS OF A LARGE EARTHQUAKE FROM THE RELATED SMALL EARTHQUAKE ONES

(1) Relation between the spectra of a large earthquake and of the related small ones as a point source

As described above, earthquake motions $f(t)$ at a given site result principally from source characteristics, propagation path of waves and local site conditions. Now let $F(\omega)$ be the Fourier transform for $f(t)$, and then assuming that the above three factors are linear, $F(\omega)$ is expressed as follows:

$$F(\omega)=I(\omega)\cdot G(\omega)\cdot R(\omega)\cdot S(\omega), \quad (1)$$

where $I(\omega)$ means the frequency characteristics of instrument, $G(\omega)$ frequency response function of local soil conditions, $R(\omega)$ frequency response function of propagation media of waves, $S(\omega)$ source spectrum, and ω circular frequency.

We here consider a large earthquake (mainshock) m and its related small earthquake (foreshock or aftershock) e as shown in Fig. 1. Denoting m and e to the large earthquake motions and small ones, respectively, the following expressions are derived from Eq. (1):

$$F_m(\omega)=I(\omega)\cdot G_m(\omega)\cdot R_m(\omega)\cdot S_m(\omega), \quad (2)$$

$$F_e(\omega)=I(\omega)\cdot G_e(\omega)\cdot R_e(\omega)\cdot S_e(\omega). \quad (3)$$

As well known, mainshock and its related small shock are considered to occur in almost the same region and the earthquake waves owing to the both shocks travel through almost the same media, in particular, near the observation site. Accordingly, if we assume that the local soil layers have little material non-linearity, we can regard that $G_m(\omega)$ and $G_e(\omega)$ are equal to each other, and the following expression is obtained from Eqs. (2) and (3):

$$F_m(\omega)=F_e(\omega)\cdot\frac{R_m(\omega)\cdot S_m(\omega)}{R_e(\omega)\cdot S_e(\omega)}. \quad (4)$$

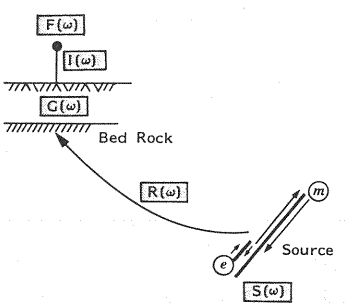

Fig. 1 Schematic profile for earthquake ground motions.

(2) Source spectra due to faulting source model composed of several sub-faults

Eq. (4) is a spectra relation which is satisfied in the case of a point source. As described in the preceding, however, earthquakes are due to fault slips, and hence it is necessary to extend the source spectrum $S_m(\omega)$ in Eq. (4) to fault source. It has been shown from recent studies on faulting mechanism that large earthquakes have a character of multiple shocks and their faults consist of several sub-faults[8]. We examine here how the point source spectrum $S_m(\omega)$ is related to the spectra resulting from successive rupture of sub-faults which are referred to as "elementary earthquakes" in this paper.

Suppose now that a large earthquake fault has the shape of rectangle composed of N sub-faults as illustrated in Fig. 2 and its overall length is much smaller than the epicentral distance. When source spectrum due to each sub-fault is expressed as $S_n(\omega)$, the resultant source spectrum $S_m(\omega)$ becomes

$$S_m(\omega)=\sum_{n=1}^{N} S_n(\omega). \quad (5)$$

Generally speaking, it would be expected that $S_n(\omega)$ $(n=1\sim N)$ are different from each other. In particular, the phase spectrum of $S_n(\omega)$ may change remarkably from element to element since faulting of each element occurs successively propagating over the overall fault plane. The amplitude spectrum of $S_n(\omega)$, on the other hand, would be less dependent on element compared with the phase spectrum even though there is a little difference. So, we rewrite Eq. (5) as follows on the assumption that the variation for the amplitude spectrum of $S_n(\omega)$ is little.

$$S_m(\omega)=\sum_{n=1}^{N} |S_0(\omega)|\, e^{-i\xi_n(\omega)}, \quad (6)$$

where $S_0(\omega)$ is the amplitude spectrum averaged for $S_n(\omega)$ $(n=1\sim N)$, $\xi_n(\omega)$ the phase spectrum for n element, and i imaginary unit.

$\xi_n(\omega)$ in Eq. (6) is considered to be determined from various causes such as propagation manner from element to element, faulting mechanism of each element and so on. But the inhomogeneous dynamic faulting theory[9] indicates that it is determined incoherently and each of $\xi_n(\omega)$ varies independently from a statistical standpoint. Thus the expected value of amplitude for $S_m(\omega)$ may be given by considering the root mean square of Eq. (6) as follows.

$$E[|S_m(\omega)|]=\sqrt{N}\,|S_0(\omega)|, \quad (7)$$

where $|\cdot|$ means absolute value and $E[\ ]$ expected value.

(3) Synthesis of a large earthquake spectrum from small earthquake ones with aid of faulting model

In this section, Eq. (4) which was derived as a point source is extended to faulting model by using the relation of Eq. (7). As shown in Fig. 3, we now consider that the mainshock has a rectangular fault and is

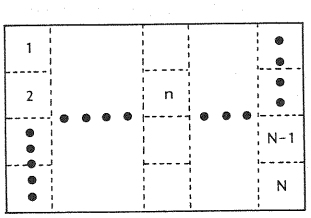

Fig. 2 Rectangle fault model.

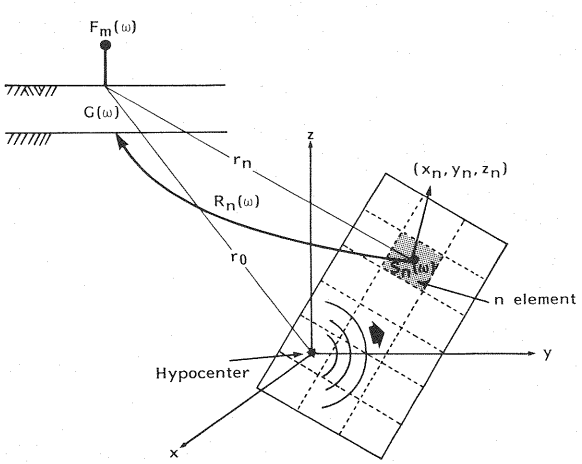

Fig. 3 Earthquake ground motions due to fault model.

composed of N elementary earthquakes. Then, writing the source spectrum and frequency response function of wave path, which will be called "wave path spectrum" hereafter, due to the n-th element as $S_n(\omega)$ and $R_n(\omega)$, respectively, the term $R_m(\omega)\cdot S_m(\omega)$ in Eq. (4) is given by

$$R_m(\omega)\cdot S_m(\omega)=\sum_{n=1}^{N} R_n(\omega)\cdot S_n(\omega). \quad (8)$$

Here, we place the origin of the Cartesian co-ordinates at the initiating point of rupture which is r_0 away from the observation site, as illustrated in Fig. 3. Furthermore, it is assumed that the rupture propagates from the origin in all directions with uniform velocity v. Using the above conditions and assuming the uniformity about the amplitude spectrum mentioned in the preceding section, the elementary source spectrum $S_n(\omega)$ is expressed as

$$S_n(\omega)=|S_0(\omega)|\cdot e^{-i\Phi_n(\omega)}\cdot e^{-i\omega\sqrt{x_n^2+y_n^2+z_n^2}/v}, \quad (9)$$

where $|S_0(\omega)|$: source amplitude spectrum averaged for all elements, (x_n, y_n, z_n) : co-ordinates of the center of n element, $\phi_n(\omega)$: phase angle except the propagation effect of rupture.

The wave path spectrum $R_n(\omega)$, meanwhile, may be also treated in the same way as $S_n(\omega)$. That is, its absolute value would show little change along with element, and if any, it mainly depends on the distance between the observation site and the element concerned because the path media for the whole elements are almost the same. So, $R_n(\omega)$ may be written as

$$R_n(\omega)=|R_0(\omega, r_n)|\cdot e^{-i\psi_n(\omega)}\cdot e^{-i\omega\frac{r_n-r_0}{\beta}}, \quad (10)$$

where $|R_0(\omega, r_n)|$: representative amplitude spectrum of wave path spectrum, β : propagation velocity of earthquake wave, r_n : distance between the center of n element and the observation site, $\psi_n(\omega)$: phase angle peculiar to $R_n(\omega)$.

Similarly, the small earthquake spectra $R_e(\omega)$ and $S_e(\omega)$ in Eq. (4) can be expressed as follows separating their amplitude and phase :

$$R_e(\omega)=|R_e(\omega)|\cdot e^{-i\eta_e(\omega)}, \quad (11) \qquad S_e(\omega)=|S_e(\omega)|\cdot e^{-i\zeta_e(\omega)}. \quad (12)$$

By substituting Eqs. (8), (9), (10), (11) and (12) into Eq. (4) in consideration of the relation Eq. (7), we get

$$F_m(\omega)=F_e(\omega)\frac{1}{\sqrt{N}}\sum_{n=1}^{N}\frac{|R_0(\omega, r_n)|\cdot E[|S_m(\omega)|]}{|R_e(\omega)|\cdot|S_e(\omega)|}\cdot e^{-i\omega\left(\frac{r_n-r_0}{\beta}+\frac{\sqrt{x_n^2+y_n^2+z_n^2}}{v}\right)}\cdot e^{-i\Phi_n(\omega)}, \quad (13)$$

where $\Phi_n(\omega)=\phi_n(\omega)+\psi_n(\omega)-\eta_e(\omega)-\zeta_e(\omega)$.

As a rule, a mainshock and its related small shocks such as foreshocks and aftershocks may resemble each other in their source spectra since they are due to similar focal mechanism[8]. Therefore, we here assume that there is a scaling law for the source spectra of these shocks and moreover that the law is chiefly determined by earthquake magnitude M and focal depth D. From these assumptions, we write as

$$\frac{E[|S_m(\omega)|]}{|S_e(\omega)|}=\frac{|S(\omega, M_m, D_m)|}{|S(\omega, M_e, D_e)|}, \quad (14)$$

where the subscripts m and e mean, respectively, mainshock and its related small shock.

On the other hand, both seismic weves due to the elementary earthquakes of the mainshock and due to its related small shock are considered to travel through almost the same media, and so $|R_e(\omega)|$ and $|R_0(\omega, r_n)|$ in Eq. (13) may be expressed as an identical function. That is,

$$\frac{|R_0(\omega, r_n)|}{|R_e(\omega)|}=\frac{|R(\omega, r_n)|}{|R(\omega, r_e)|}, \quad (15)$$

where r_e is the distance between the hypocenter of the small shock and observation site. The substitution of Eqs. (14) and (15) into Eq. (13) gives

$$F_m(\omega)=F_e(\omega)\frac{1}{\sqrt{N}}\sum_{n=1}^{N}\frac{|R(\omega, r_n)|\cdot|S(\omega, M_m, D_m)|}{|R(\omega, r_e)|\cdot|S(\omega, M_e, D_e)|}\cdot e^{-i\omega\left(\frac{r_n-r_0}{\beta}+\frac{\sqrt{x_n^2+y_n^2+z_n^2}}{v}\right)}\cdot e^{-i\Phi_n(\omega)}. \quad (16)$$

Eq. (16) is a semi-empirical expression, which was derived by incorporating the point source model with the faulting source model, for synthesizing strong-motion spectra during a large earthquake from its related small earthquake ones. In order to execute Eq. (16) effectively, it is necessary to make clear some characteristics about the scaling law of source spectra and wave path spectra, the number N of elementary earthquakes, and so on.

3. A SCALING LAW OF SPECTRA AND FAULTING PATTERN OF EARTHQUAKE BY STATISTICAL ANALYSES OF STRONG-MOTION ACCELEROGRAMS

There may be several ways from theoretical to statistical for the purpose of obtaining spectral shapes in accordance to earthquake size. For example, it would be possible to discuss earthquake spectra theoretically by using a law to scale the faulting parameters such as fault length, maximum slip, rise time, and the like which have been completed on assumption of the so-called uniform slip model[10]. Our goal in this study, however, is to obtain a scaling law in terms of acceleration motions. As well known, the uniform slip model is not necessarily suitable to acceleration motions. For this reason we employ an another way in which strong-motion accelerograms observed in the past are analyzed statistically and a statistical scaling law of acceleration spectra is derived.

Strong-motion accelerograms have been generally obtained at the ground surface. As described previously, however, local soil conditions peculiar to the observation site exert a great influence on such surface accelerograms. This means that we must remove the effect due to the local conditions from these accelerograms to detect spectral characteristics belonging to earthquake sources. The author presented a statistical technique by which amplification spectra owing to individual observation site, source spectra and wave path spectra can be obtained separately from the surface spectra when many accelerograms are available at several sites under various earthquake circumstances[5),11)]. On condition that L observation sites are prepared in all, the statistical expression is

$$\log_{10} V(\omega)=a(\omega)M^2+b(\omega)M+c(\omega)D+d(\omega)\log_{10}(r+30)+e(\omega)+\sum_{j=1}^{L-1}A_j(\omega)\cdot S_j, \quad \cdots\cdots (17)$$

where $V(\omega)$: earthquake spectrum, M : earthquake magnitude, D : focal depth, r : source-to-observation site distance, S_j : dummy variable, $a(\omega)$, $b(\omega)$, ……, $A_j(\omega)$: regression coefficients.

The background of Eq. (17) was explained in detail in Refs. 5) and 10). In a word, Eq. (17) is such a multiple regression model that earthquake spectra are analyzed statistically by the three factors-source characteristics, wave path and individual local site condition which are represented simply by magnitude and focal depth, source-to-station distance, and dummy variable, respectively. Although Eq. (17) is a statistical model and Eq. (1) an analytical one, both have the following relations for each term :

$$|F(\omega)|\equiv V(\omega), \quad \cdots\cdots (18) \qquad |R(\omega)|\equiv(r+30)^{d(\omega)}, \quad \cdots\cdots (19)$$

$$|G(\omega)|\equiv 10^{A_j(\omega)}, \quad \cdots\cdots (20) \qquad |S(\omega)|\equiv 10^{a(\omega)M^2+b(\omega)M}\cdot 10^{c(\omega)D}\cdot 10^{e(\omega)}. \quad \cdots\cdots (21)$$

From the equivalent relations of Eqs. (19) and (21), we can get the scaling laws of source spectra and wave path spectra necessary to Eq. (16) as follows :

$$\frac{|S(\omega, M_m, D_m)|}{|S(\omega, M_e, D_e)|}=10^{a(\omega)(M_m^2-M_e^2)+b(\omega)(M_m-M_e)}\cdot 10^{c(\omega)(D_m-D_e)}, \quad \cdots\cdots (22)$$

$$\frac{|R(\omega, r_n)|}{|R(\omega, r_e)|}=\left(\frac{r_n+30}{r_e+30}\right)^{d(\omega)}, \quad \cdots\cdots (23)$$

where the subscripts m and e signify mainshock and its related small shock each.

As an example, Eqs. (22) and (23) are estimated, respectively, as shown in Figs. 4 and 5 by using the regression coefficients $a(\omega)$, $b(\omega)$, $c(\omega)$, and $d(\omega)$ which were obtained statistically from 228 strong-motion accelerograms in Japan[5)]. Fig. 4 shows the values of Eq. (22) when M_m is varied from 6.5 to 8.0 on condition of M_e=6.0, D_e=30 km and D_m=30 km. Also Fig. 5 is the values of Eq. (23) calculated by varying r_n from 20 to 150 km while keeping r_e=50 km. As indicated in Figs. 4 and 5, we can get easily the

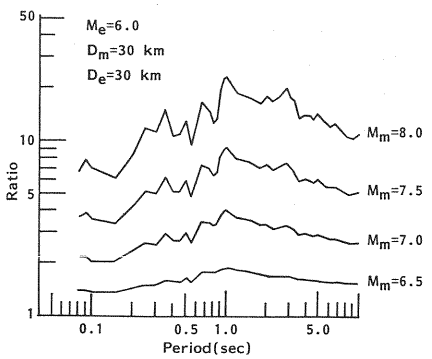

Fig. 4 Examples of source spectra ratio.

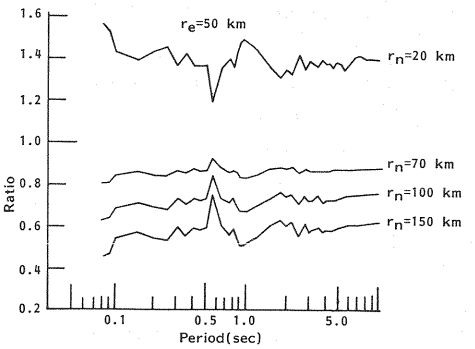

Fig. 5 Examples of wave path spectra ratio.

spectra ratios involved in Eq. (16) provided that such familiar earthquake factors as magnitude, focal depth and source-to-station distance are available.

On the other hand, the total number N to be counted for elementary earthquakes in Eq. (16) would also have an effect on the results of $F_m(\omega)$ to such an extent as the spectra ratios do. Probably it is associated closely with the heterogeneity in earthquake fault plane and may be nearly equivalent to the total number of the localized cracks characterized by the specific barrier model[9]. In order to clarify the general aspects of the localized cracks over earthquake fault, the author investigated a scaling law peculiar to the cracks by relating the statistical results mentioned in Eq. (17) with the specific barrier model of faulting[5]. It was made clear from the investigation that both characteristic lengths of the whole fault and of the localized crack for an earthquake are scaled in a rather similar way by earthquake magnitude and therefore that the total number of cracks over the whole fault is relatively stable irrespective of earthquake magnitude M, ranging from 10 to 20 between $M=6$ and $M=8$. The mean value of the total cracks number estimated statistically from $M=6$ to $M=8$ is nearly equal to 16. It is of interest that we statistically obtained such a simple result concerning localized cracks, despite of the complicated phenomena expected in heterogeneous faulting. Anyway, we can apply effectively the above result to Eq. (16), that is, N would be set to be 16 regardless of earthquake magnitude M in the following.

$\Phi_n(\omega)$ in Eq. (16), meanwhile, is due to the phase angle of spectrum special to individual elementary earthquake on the fault as well as its related small shock, as described in Eq. (13). It may change at random from element to element reflecting the complicated faulting mechanism, and so it would be relevant that we regard it as a stochastic variable rather than deterministic one. In this paper, accordingly, $\Phi_n(\omega)$ $(n=1\sim N)$ are varied as the uniform pseude-random numbers of $0\sim 2\pi$ for each element and moreover are dealt with to be constant irrespective of ω because of the computation technique in the FFT.

Now that the principal terms in Eq. (16) were given as described above, we can synthesize the accelerogram for a given mainshock by operating the inverse Fourier transform for $F_m(\omega)$ in the equation.

As mentioned above, the present method is not based on the scaling law of earthquake moment but on the statistical scaling law of spectra in terms of earthquake magnitude. On the other hand, long period motions of ground are considered to be dependent on earthquake moment, so the application of the present method may be confined to acceleration motions which are supposed to be independent of earthquake moment.

4. PREDICTION EXAMPLE OF STRONG-MOTION ACCELEROGRAM FROM SMALL EARTHQUAKE RECORD

In order to examine the validity of the above method for predicting strong-motion accelerograms, we applied it to several earthquakes occurred in Japan and compared the predicted results with the observed records. In this paper we show the results of two representative earthquakes on account of space consideration. In the following, a mainshock is assumed from the above consideration to have a rectangular

fault consisting of sub-faults of 16 in all. Also the sub-faults are assumed to be not only uniform but also similar in shape to the overall fault. On the other hand, the rupture velocity v of faulting is assumed to be 2.5 km/s and 3.0 km/s, respectively, for the intra-plate earthquake and the interplate earthquake, referring to Geller's study[10]. The earthquake wave velocity β is also set according to Geller's expression $v/\beta=0.72$ as well as the above value of v. In addition to these constants, the rupture front over fault is assumed to propagate with the constant velocity in all directions. Although these constants and propagation manner of rupture front vary in accordance with earthquakes, they are set to be uniform in this paper because their variations due to the difference of earthquakes may be small compared with the ones of the spectra ratio.

(1) The 1983 Nihonkai-chubu earthquake

Fig. 6 shows the origins of the mainshock and representative aftershocks of the 1983 Nihonkai-chubu earthquake together with the principal sites which observed the accelerograms due to these shocks. The fault which was deduced from the distribution[12] of aftershocks is also shown in Fig. 6. The earthquake factors for the mainshock and aftershocks are listed on Table 1. The fault parameters fo the mainshock are summarized in Table 2 so as to apply to the prediction method presented here. In Table 2, the dip angle and dip direction were quoted from Sato et. al.[13] and the other parameters were deduced by the author. Fig. 7 is the accelerogram obtained at Akita site during the aftershock e_1. By emloying the Fourier transform of the accelerogram as $F_e(\omega)$ in Eq. (16) and using the parameters in Tables 1 and 2, the accelerogram during the mainshock was synthesized as shown in Fig. 8. In Fig. 8 the record obtained during the mainshock is also drawn for comparison. We can see from Fig. 8 that the synthesized accelerogram is consistent comparatively well with the observed one in the points of amplitude and duration. Fig. 9

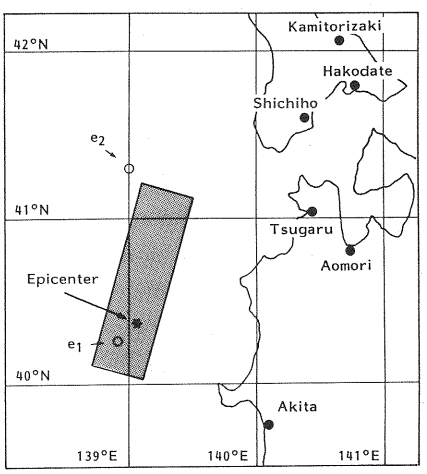

Fig. 6 The map showing the 1983 Nihonkai-chubu earthquake.

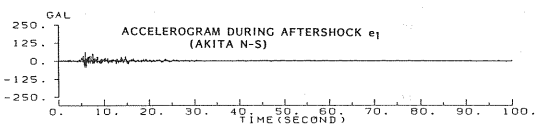

Fig. 7 The accelerogram at Akita site during the aftershock e_1.

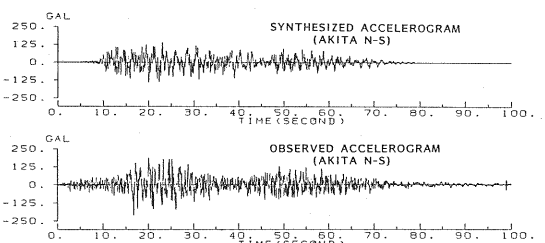

Fig. 8 Comparison between the synthesized accelerogram and observed one at Akita site during the mainshock.

Table 1 The earthquake factors of the 1983 Nihonkai-chubu earthquake.

	Date	Magnitude	Depth (km)	Epicentral Distance (km)	
Mainshock m	May 26,1983	7.7	14.0	(Akita)	107.0
				(Aomori)	156.0
				(Hakodate)	211.0
				(Tsugaru)	137.0
				(Shichiho)	177.0
				(Kamitorizaki)	236.0
Aftershock e1	June 9,1983	6.1	23.0	(Akita)	113.0
Aftershock e2	June 21,1983	7.1	6.0	(Aomori)	160.0
				(Hakodate)	155.0
				(Tsugaru)	129.0
				(Shichiho)	123.0
				(Kamitorizaki)	169.0

Table 2 The fault parameters of the 1983 Nihonkai-chubu earthquake.

Fault Length	125 km
Fault Width	35 km
Center of Fault	40.61°N 139.11°E Depth:14 km
Dip Angle	20°
Dip Direction	N105°E
Division of Fault N	16 (4x4)
Velocity of Fault Rupture	2.5 (km/sec)
Velocity of Earthquake wave	3.5 (km/sec)

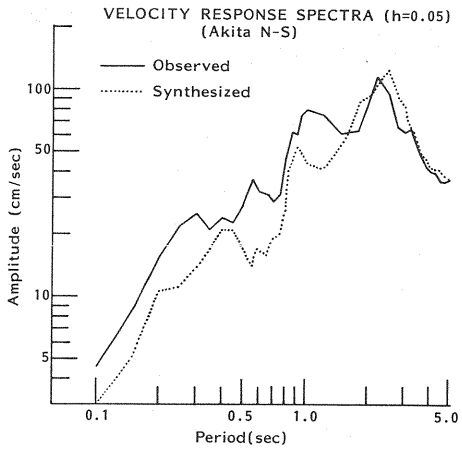

Fig. 9 Comparison of the spectra calculated from the accelerograms of Akita site.

indicates the spectra calculated from the synthesized and observed accelerograms. It is seen in Fig. 9 that both of the synthesize and the observed agree relatively well not only in amplitude and duration but also in spectral characteristics.

Similar results to Fig. 8 are shown in Fig. 10 for the other observation sites. It should be noted in Fig. 10 that the accelerograms due to the aftershock e_2 were used as the small earthquake records. We can also find in Fig. 10 that there is a good consistence between the synthesized accelerograms and observed ones. The 1983 Nihonkai-chubu earthquake was pointed out from some studies[12] to be a special multiple shock which is composed of two main events located in the southern and northern parts of the fault shown in Fig. 6. But, the method presented here followed well the accelerograms owing to such a characteristic event, as shown above. It would be emphasized therefore that this method is applicable to a complicated earthquake even though some simplicities are involved in it.

(2) The 1978 Miyagiken-oki earthquake

Fig. 11 shows the origins of the shocks related with the 1978 Miyagiken-oki earthquake. In Fig. 11, the fault[14] which was estimated from the distribution of the aftershocks is also indicated with the representative observation sites where accelerograms were obtained during the mainshock. Being different from the 1983 Nihonkai-chubu earthquake, this earthquake provided the

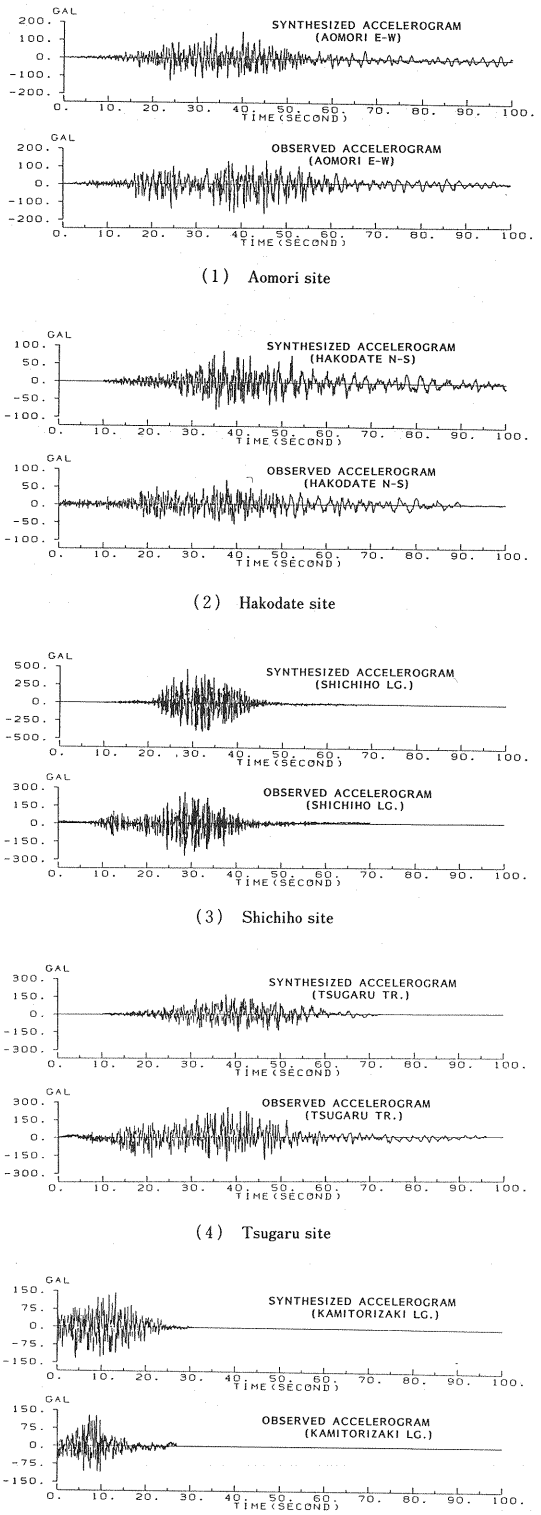

Fig. 10 Comparison between the synthesized accelerogams and observed ones during the mainshock.

observation sites with no accelerogram due to the aftershocks occurred in the fault area in Fig. 11. As explained in the preceding, the present method needs the accelerogram produced by a small event equivalent to the elementary earthquake over mainshock fault. Here, in order to investigate the applicability of the method in the case of not satisfying this condition, we attempt to estimate theoretically the accelerograms during the mainshock by using the accelerograms due to a shock e which is apart from the fault area as shown in Fig. 11.

The earthquake factors for these shocks and the fault parameters[14] are, respectively, summarized on Tables 3 and 4. The acceleration waves, which were synthesized for the three observation sites by using the parameters as well as the records due to the shock *e*, are shown in Fig. 12 being compared with the observed accelerograms. Also, Fig. 13

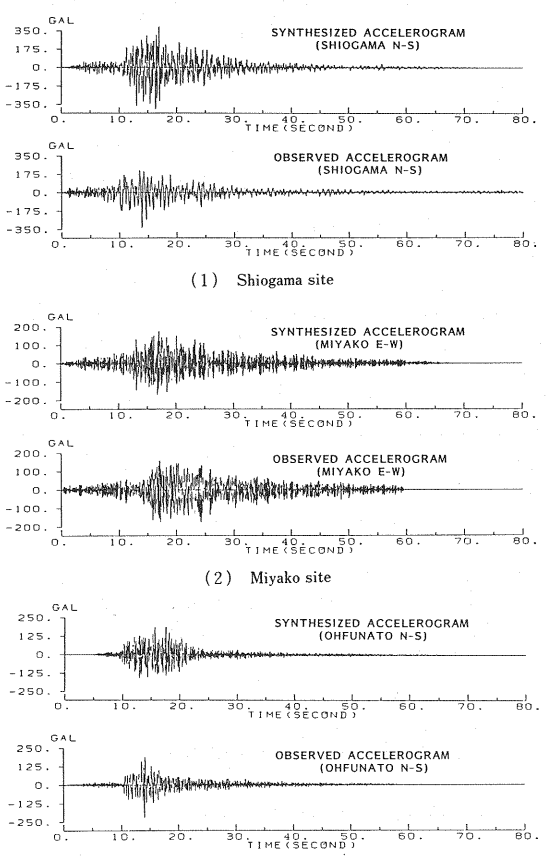

Fig. 12 Comparison between the synthesized accelerograms and observed ones during the mainshock.

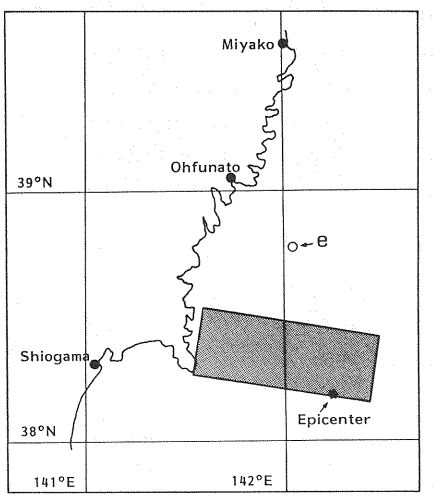

Fig. 11 The map showing the 1978 Miyagiken-oki earthquake.

Table 3 The earthquake factors of the 1978 Miyagiken-oki earthquake.

	Date	Magnitude	Depth (km)	Epicentral Distance (km)
Mainshock m	June 12, 1978	7.4	30.0	(Shiogama) 100.0 (Ohfunato) 103.0 (Miyako) 166.0
Shock e	Feb. 20, 1978	6.7	56.0	(Shiogama) 101.0 (Ohfunato) 39.5 (Miyako) 88.2

Table 4 The fault parameters of the 1978 Miyagiken-oki earthquake.

Fault Length	80 km
Fault Width	30 km
Center of Fault	38.33°N 142.00°E Depth:38.5 km
Dip Angle	20°
Dip Direction	N80°W
Division of Fault N	16 (4×4)
Velocity of Fault Rupture	3.0 (km/sec)
Velocity of Earthquake Wave	4.2 (km/sec)

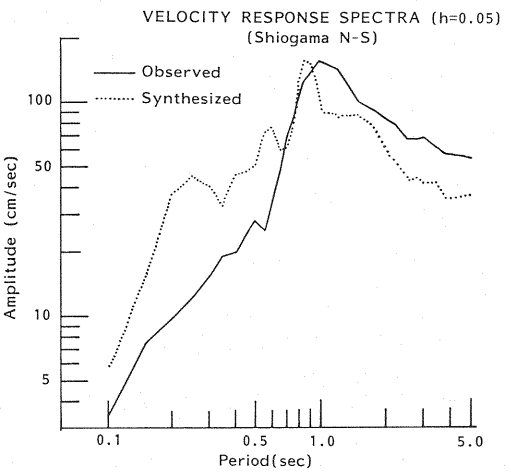

Fig. 13 Comparison of the spectra calculated from the accelerogams of Shiogama site.

shows, as an example, the respones spectra calculated from the accelerograms of Shiogama site. We can see from Figs. 12 and 13 that the synthesized results agree relatively well with the observed ones even in this earthquake. While the small earthquake used here has no strict condition necessary to estimate as mentioned above, the synthesized results explain well the observed ones. It would be pointed out from this indication that the present method needs relatively less strictness in selecting small earthquake records for the synthesis.

5. CONCLUDING REMARKS

In this study we have derived a simplified semi-empirical method for predicting strong-motion accelerogram from small earthquake records. The important terms constitutinhg this method are the scaling law of spectra and the number of sub-faults. They were obtained statitically in this paper from the past strong-motion accelerograms in Japan. Although this method requires merely such simple source parameters as earthquake magnitude, focal depth, source-to-station distance, and geometric shape of fault, it was shown that the accelerograms predicted by the method are consistent relatively well with the observed ones. Also the method was confirmed to have a versatility when selecting small earthquake records. It would be thus concluded that the method presented here is an effective tool for predicting strong-motion accelerograms.

Acknowledgements

The accelerograms used in this study were available from the Port and Harbour Research Institute of Ministry of Transport and the Public Works Research Institute of Ministry of Construction. The author thanks the concerned people of the both institutes for providing these useful accelerograms.

REFERENCES

1) Inoue, R. : Studies on design earthquakes in the period range of 2 to 20 sec—a review, Proc. of JSCE, No. 374/ I -6, pp. 1~23, 1986 (in Japanese).
2) Aki, K. : Strong-motion seismology, Proceeding of the International School of Physics ENRICO FERMI, pp. 223~250, 1983.
3) Hartzell, S. H. : Earthquake aftershocks as Green's functions, Geophys. Letters, Vol. 5, No. 1, pp. 1~4, 1978.
4) Iida, M. and Hakuno, M. : The synthesis of the acceleration wave in a great earthquake by small earthquake records, Proc. of JSCE, No. 329, pp. 57~68, 1983 (in Japanese).
5) Kamiyama, M. : Earthquake source chatacteristics inferred from the statistically analyzed spectra of strong motions with aid of dynamic model of faulting, Proc. of JSCE, No. 386/ I -8, pp. 175~184, 1987.
6) Irikura, K. : Prediction of strong acceleration motions using empirical Green's function, Proc. of the 7-th Japan Earthquake Engineering Symposium, pp. 151~156, 1986.
7) Takemura, M. and Ikeura, T. : Semi-empirical synthesis of strong ground motions for the description of inhomogeneous faulting, Zisin, Ser. 2, 40, pp. 77~88, 1987 (in Japanese with English abstract).
8) Trifunac, M. D. and Brune, J. N. : Complexity of energy release during the Imperial Valley California, earthquake of 1940, BSSA, Vol. 60, No. 1, pp. 137~160, 1970.
9) Papageorgiou, A. S. and Aki, K. : A specific barrier model for the quantitative description of inhomogeneous faulting and the prediction of strong ground motion Part I and Part II, BSSA, Vol. 73, pp. 693~722, pp. 953~978, 1983.
10) Geller, R. J. : Scaling relations for earthquake source parameters and magnitudes, BSSA, Vol. 66, No. 5, pp. 1501~1523, 1976.
11) Kamiyama, M. and Yanagisawa, E. : A statistical model for estimating response spectra of strong earthquake ground motions with emphasis on local soil conditions, Soils and Foundations, Vol. 26, No. 2, pp. 16~32, 1986.
12) Hirasawa, T. : The characteristics of the earthquake and earthquake motions, in Report on the Damage Investigations of the 1987 Nihonkai-chubu Earthquake, Tohoku Branch of the Japanese Society of Soil Mechnics and Foundation Engineering, pp. 11~20, 1986 (in Japanese).
13) Sato, T., Kosuga, M. Tanaka, K. and Sato, Y. : Aftershocks distribution of the 1983 Nihonkai-chubu earthquake, Report of Natural Disaster Research in the Tohoku District, Vol. 20, pp. 1~6, 1984 (in Japanese).
14) Hirasawa, T. : Seismic activity, in General Report on the 1978 Miyagi-Oki Earthquake, Tohoku Branch of Japan Civil Eng. pp. 7~28, 1980, (in Japanese).

(Received March 9 1987)